Hugoniot Measurements for Laser-Generated Shock Waves in Aluminum

A. Ng, D. Parfeniuk, and L. DaSilva
Physics Department, University of British Columbia, Vancouver, British Columbia V6T 2A6, Canada
(Received 14 January 1985)

We report on the first experimental measurement of principal Hugoniots in aluminum for shock pressures of 0.3–12 Mbar generated by laser-driven ablation. These were derived from independent measurements of the shock speed, shock pressure, and shock-heated target temperature. The results showed excellent agreement with LASNEX simulations and with calculations using SESAME equation-of-state data. More importantly, the results indicated that the shock speed and temperature Hugoniot may provide useful equation-of-state studies in laser-generated shock-wave experiments.

PACS numbers: 52.50.Jm, 52.35.Tc, 62.50.+p

The equation of state of matter at high pressure, temperature, and density is of great importance to the study of many phenomena in geophysics, planetary physics, high-density plasmas, nuclear explosions, and inertial fusion. At low temperatures, accurate equations of state for high-density matter can be derived from band-structure calculations[1–3] whereas at sufficiently high pressures all statistical models (Thomas-Fermi,[4,5] Thomas-Fermi-Dirac,[6] Thomas-Fermi-Kirzhnitz,[7–9] and quantum-statistical model[10,11]) also become accurate. However, in intermediate regimes of pressure ($\lesssim 10^3$ Mbar) and temperature ($\gtrsim 1$ eV), experimental measurements are needed to corroborate theoretical predictions. Since dynamic pressures exceeding multimegabars can be readily attained in solids via shock waves, equation-of-state data are generally derived from Hugoniot measurements.[12] With use of shocks generated by nuclear explosions, accurate benchmark data have been obtained from the measurement of an absolute Hugoniot point[13] as well as from impedance-matching measurements.[14] On the other hand, ultrahigh-pressure shock waves can also be effectively produced in laboratory experiments by laser-driven ablation.[15–19] This has led to a strong interest in obtaining Hugoniot measurements in laser-target interactions.[20]

Here, we report on the first experimental measurement of principal Hugoniots in a laser-irradiated planar aluminum target. These were derived from independent measurements of shock speed, shock pressure, and the temperature of the shock-heated target. The measured shock-speed and pressure and the shock-speed and temperature Hugoniots both showed excellent agreement with LASNEX simulations[21] as well as calculations using the SESAME equation of state.[22] Experimental accuracy in determining the shock-speed and pressure Hugoniot severely limits its use in equation-of-state studies. However, because of its much greater sensitivity to equation of state, the measured temperature and shock-speed Hugoniot showed sufficient accuracy to be considered as an important means for obtaining equation-of-state data in laser-generated shock-wave experiments.

In this experiment, planar aluminum targets (typically 15×15 mm^2 with thicknesses ranging from 10 to 50 μm) were irradiated with a 0.53-μm, 2-ns (full width at half maximum) laser pulse. The laser beam was focused onto the target with $f/10$ optics at an incident angle of 10° off target normal. At focus, the intensity distribution is nearly Gaussian with 90% of the incident laser energy contained in a spot of 80 μm diameter and 60% in a spot of 40 μm diameter. Accordingly, the irradiance averaged over the central region containing 60% of the laser energy (Φ_{60}) was higher than that averaged over the 90%-energy area (Φ_{90}) by a factor of ~ 2.7. Time-resolved (30 ps resolution) measurements showed spatial intensity modulations (4 μm resolution) of $< 30\%$ whereas time-integrated measurements revealed modulations of $< 10\%$. Details of the experimental setup have been described earlier.[23] Maximum absorbed irradiance was $\Phi_{90} \leq 7\times 10^{13}$ W/cm^2.

The shock speed in aluminum was determined from the shock transit times through targets of various thicknesses. The rear surface of the target was imaged onto the slit of a Hamamatsu C1370 streak camera with $f/4$ optics at an observation angle of 12° with respect to target normal. The luminescence of the target rear surface due to the shock breakout was recorded as a function of time. In this measurement, the luminescent intensity was observed through a 100-Å bandpass filter centered at 5700 Å. The shock transit time was obtained by comparison of the time for shock breakout to the laser fiducial which was simultaneously recorded by the streak camera. Details of these measurements have been reported.[24] The shock was observed to emerge at the target rear surface in a region of ~ 40 μm diameter. This is consistent with the higher intensity, central region of the focal spot which contains 60% of the incident laser energy. The rise time of the shock-induced luminescence varied from 100 to 300 ps. No rear-surface luminescence was detected prior to the shock arrival, this indicating the absence of any significant target preheat. Figure 1 shows the measured shock transit time as a function of target thickness for an absorbed irradiance of

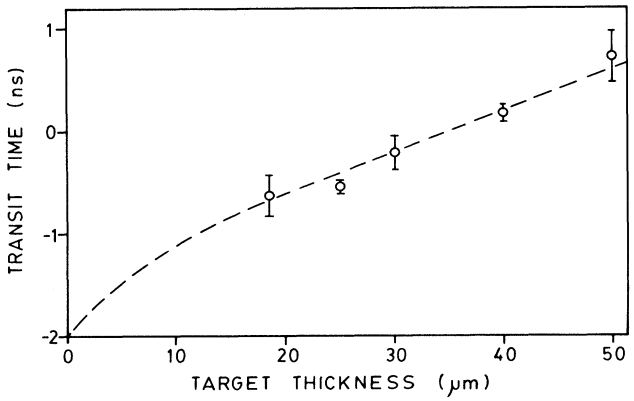

FIG. 1. Shock transit time as a function of target thickness for an absorbed irradiance of $\Phi_{60}=1\times10^{14}$ W/cm^2: circles, measured data; dashed line, result of one-dimensional simulations. Time zero corresponds to the time of peak laser intensity.

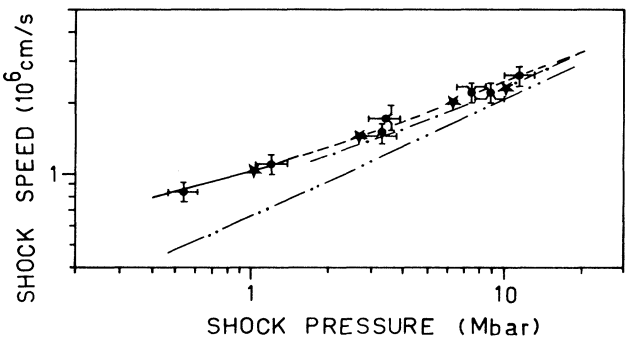

FIG. 2. Shock-speed and pressure Hugoniot for aluminum: solid circles, measured data; solid line, Mitchell and Nellis; dashed line, SESAME; dot-dashed line, Thomas-Fermi; double-dot–dashed line, ideal gas; stars, LASNEX simulations.

$\Phi_{90}\simeq4\times10^{13}$ W/cm^2 or $\Phi_{60}\simeq1\times10^{14}$ W/cm^2. The linear trajectory indicates that the shock wave reached a quasisteady state before it propagated 19 μm into the target, and remained steady and planar to 50 μm. The slope of this graph then yielded a steady-shock speed of $(2.2\pm0.2)\times10^6$ cm/s. The trajectory of the shock front propagating in an aluminum target was also calculated with a one-dimensional hydrodynamic code MEDUSA.[25] The result corresponding to an absorbed irradiance, $\Phi_{60}=1\times10^{14}$ W/cm^2, is also included in Fig. 2 which shows good agreement with the experimental data. (Φ_{60} is used because the shock broke out in a region of ~40 μm diameter, as noted above.) The measurement of shock speed was repeated for different absorbed irradiances with $\Phi_{60}\simeq3\times10^{12}$–$2\times10^{14}$ W/cm^2.

The corresponding ablation pressures were inferred from ion expansion measurements on the target front side. Because of the finite transit time, the ablation pressure may not be exactly the same as the pressure at the shock front at any instant. In a long-pulse experiment, however, the laser-driven ablation is nearly steady state and the shock pressure is essentially equal to the ablation pressure.[26] Details of the ion measurement and the results have been reported previously.[27] By combination of these results with that from the shock-speed measurements, a principal Hugoniot of shock speed and pressure could be obtained. This is presented in Fig. 2. Also shown are the experimental results of Mitchell and Nellis,[28] results of LASNEX simulations, and the results of shock calculations[29] using the ideal gas, Thomas-Fermi[4,5] or the SESAME[22] equations of state for aluminum. In the lower pressure range, our results are in good agreement with that of Mitchell and Nellis where the shock waves were generated using a two-stage gas gun. Our data also showed excellent agreement with both LASNEX simulations and calculations using the SESAME equation of state. Although the data clearly verified the well-known inadequacy of the ideal-gas equation of state, they could not discriminate against the also inadequate Thomas-Fermi equation of state because of the limited experimental accuracy.

It should be noted that the excellent agreement of the measured Hugoniot of shock speed and pressure with theory could be fortuitous since the shock speed was determined from a spatially and temporally resolved measurement whereas the shock pressure was a global, time- and space-averaged quantity derived from the kinetic energy and velocity of the ablatively driven, expanding plasma ions. The difference might have been smaller than the experimental accuracy which also included the shot-to-shot fluctuations. Although the measured Hugoniot provides an experimental verification of the scaling of shock speed with pressure, it does not appear to be suitable for equation-of-state studies.

The temperature of the target due to shock heating was obtained from measurements of the target rear-surface luminescence.[30] Both the spectral (4200–6900 Å) and the brightness (5700 Å) temperatures were obtained. Details of the diagnostics are described elsewhere.[24] For spectral temperature measurements, the target rear surface was imaged through a prism onto the slit of the streak camera. This yielded the time-resolved luminescent spectrum from 4200 to 6900 Å. To analyze the spectral data, an integration time of 200 ps was used because of the low signal intensity and this set an effective temporal resolution. The spectral temperature was then determined by comparison of the spectrum to blackbody curves. Figure 3 shows a typical time history of the rear surface temperature. The peak temperature was taken to be the shock-heated temperature of the target. The rise time of the shock heating was generally 100–300 ps and the rear surface temperature remained nearly constant for 100–600 ps

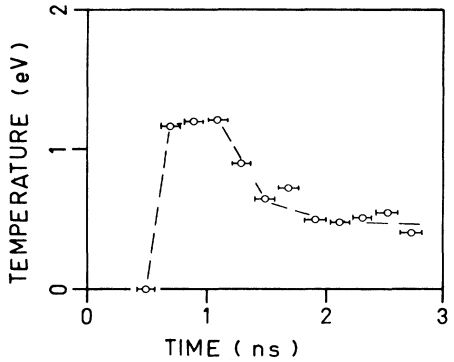

FIG. 3. Rear-surface temperature as a function of time for a 38-μm aluminum target at an absorbed irradiance of $\Phi_{60} = 5 \times 10^{13}$ W/cm^2. Time zero corresponds to the time of peak laser intensity.

before dropping off. The apparent persistence of the temperature might be due to the finite surface roughness (typically < 1 μm) of the aluminum target or to failure of the shock front to be perfectly parallel to the target rear surface. The drop in the rear surface temperature was caused by the shock-released and expanding material which formed a cooler and optically thick layer obscuring the shock-heated target. In fact, such shock unloading could significantly affect the measurement of the true shock-heated temperature of the target. This will be discussed later.

To verify the spectral temperature diagnostics, brightness temperature measurements were also made at 5700 Å by use of a 100-Å bandpass filter. The absolute response of the complete optical system including the imaging optics and streak camera was calibrated *in situ* and dynamically (camera in streak mode) with a tungsten light source.[24] The temperature of the tungsten filament was measured with an optical pyrometer. This allowed us to determine the absolute intensity of the rear-surface luminescence and therefore its brightness temperature. Accuracy in the brightness temperature measurement was estimated to be $\pm 50\%$. This diagnostic is also affected by shock unloading of the target rear surface.

Figure 4 shows the measured peak temperatures as a function of shock speed in aluminum. Each datum point for the brightness temperature corresponds to a single measurement whereas that for the spectral temperature represents the average of five or more measurements. The brightness temperatures show reasonable agreement with the spectral temperatures. Also included in Fig. 4 are the Hugoniots obtained from LASNEX simulations and from shock calculations[29] using the ideal-gas, Thomas-Fermi, and SESAME equations of state. Before the data can be compared with the calculated Hugoniots, one recalls that the effect of the rear-surface released material needs to be taken into account. A one-dimensional hydrodynamic code

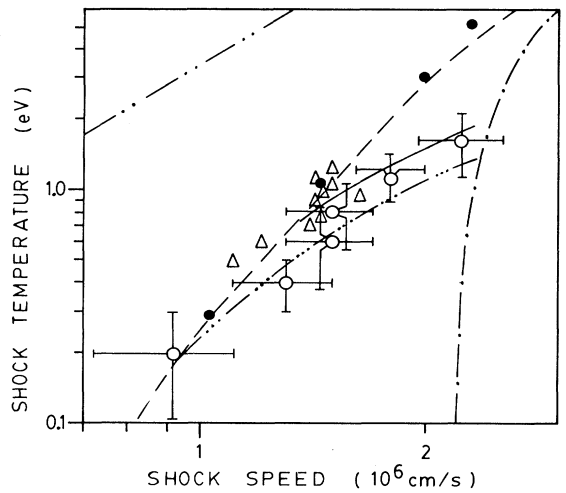

FIG. 4. Open circles, spectral temperature; triangles, brightness temperature. Shock-temperature and speed Hugoniot for aluminum: solid circles, LASNEX; dashed line, SESAME; dot-dashed line, Thomas-Fermi; double-dot–dashed line, ideal gas; triple-dot–dashed line, SESAME corrected for shock unloading of target rear surface using the SESAME opacity; and solid line, SESAME corrected for shock unloading using the bremsstrahlung absorption coefficient.

was developed including flux-corrected transport[31] and SESAME[22] equation of state to model the hydrodynamics and thermodynamics of the shocked target rear surface. To treat the absorption of the shock-induced luminous radiation by the unloading plasma, the plasma opacity needs to be included in the simulations. However, for a plasma of near solid density and low temperature (~ 1 eV), the only available data is the frequency-averaged, Roseland mean opacity from the SESAME library.[22] On the other hand, one can calculate a frequency-dependent opacity using the bremsstrahlung absorption coefficient[32] which is valid only for an ideal-gas plasma. Both of these opacities were used in the simulations while their limitations were recognized. Details of the simulations will be published elsewhere. Essentially, the density and temperature profiles in the unloading wave were determined. On the assumption that the released material radiated as a blackbody and with use of either the SESAME opacity data or the bremsstrahlung absorption coefficient, the spectral emission as observed by a detector at the target rear side was then calculated. A blackbody curve was fitted to this spectrum to yield a spectral temperature, simulating the experimental measurement. The effect of shock unloading can thus be taken into account. The modified SESAME Hugoniots are shown in Fig. 4. For temperatures $\lesssim 1$ eV, the Hugoniots are almost identical. For higher temperatures, the simulations using the bremsstrahlung absorption coefficient yielded higher spectral tempera-

tures than those using the frequency-averaged SESAME opacity. This is because of the lower opacity at all wavelengths and the increased absorption with wavelength according to the bremsstrahlung absorption calculation. In the regime of interest here, however, the differences in the calculated temperatures are relatively small and both of the corrected SESAME Hugoniots are in reasonble agreement with the data. The Hugoniot from LASNEX simulations, being almost identical to the uncorrected SESAME Hugoniot, is therefore also in excellent agreement. The data clearly reject the Hugoniots based on the ideal gas or Thomas-Fermi equations of state.

The limited availability of theoretical Hugoniot data in the literature has also restricted the comparison of our results to ideal-gas and Thomas-Fermi models, as well as SESAME data and LASNEX simulations. The advantage of using the shock-speed and temperature Hugoniot for equation-of-state studies is evident. Although the experimental accuracy achieved may not be sufficient to generate benchmark equation-of-state data, these measurements have demonstrated the feasibility of obtaining useful Hugoniot curves in a conventional laboratory experiment. The ultimate utility of the shock-speed and temperature Hugoniot will depend on the ability to improve further the accuracies of the temperature measurements as well as the opacity data.

This work is supported by the Natural Sciences and Engineering Research Council of Canada and the British Columbia Hydro and Power Authority.

[1]A. K. McMahan, B. L. Hord, and M. Ross, Phys. Rev. B **15**, 726 (1977).

[2]B. K. Godwal, S. K. Sikka, and R. Chidambaram, Phys. Rev. B **20**, 2362 (1979).

[3]F. Perrot, Phys. Rev. B **21**, 3167 (1980).

[4]R. P. Feynman, N. Metropolis, and E. Teller, Phys. Rev. **75**, 1561 (1949).

[5]R. Latter, Phys. Rev. **99**, 1854 (1955), and J. Chem. Phys. **24**, 280 (1956).

[6]R. D. Cowan and J. Ashkin, Phys. Rev. **105**, 144 (1957).

[7]D. A. Kirzhnitz, Zh. Eksp. Teor. Fiz. **32**, 115 (1957), and **35**, 1545 (1959) [Sov. Phys. JETP **5**, 64 (1957), and **8**, 1081 (1959)].

[8]N. N. Kalitkin, Zh. Eksp. Teor. Fiz. **38**, 1534 (1960) [Sov. Phys. JETP **11**, 1106 (1960)].

[9]D. A. Kirzhnitz, Yu. E. Lozovik, and G. V. Shpatakovskaya, Usp. Fiz. Nauk. **117**, 3 (1975) [Sov. Phys. Usp. **18**, 649 (1975)].

[10]N. N. Kalitkin and L. V. Kuz'mina, Fiz. Tverd. Tel. **13**, 2314 (1971) [Sov. Phys. Solid State **13**, 1938 (1972)].

[11]R. M. More, Phys. Rev. A **19**, 1234 (1979).

[12]G. E. Duvall, in *Physics of High Energy Density,* edited by P. Caldirola (Academic, New York, 1971).

[13]C. E. Ragan III, M. G. Silbert, and B. C. Diven, J. Appl. Phys. **48**, 2860 (1977).

[14]C. E. Ragan III, Phys. Rev. A **21**, 458 (1980), and **25**, 3360 (1982), and **29**, 1391 (1984).

[15]L. Veeser and J. Solem, Phys. Rev. Lett. **40**, 1391 (1978).

[16]R. J. Trainor, J. W. Shaner, J. M. Auerbach, and N. C. Holmes, Phys. Rev. Lett. **42**, 1154 (1979).

[17]L. R. Veeser, J. C. Solem, and A. J. Lieber, Appl. Phys. Lett. **35**, 761 (1979).

[18]R. J. Trainor, N. C. Holmes, R. A. Anderson, E. M. Campbell, W. C. Mead, R. J. Olness, R. E. Turner, and F. Ze, Appl. Phys. Lett. **43**, 542 (1983).

[19]F. Cottet, J. P. Romain, R. Fabbro, and B. Faral, Phys. Rev. Lett. **52**, 1884 (1984).

[20]R. M. More, in *Laser Interaction and Related Plasma Phenomena,* edited by H. J. Schwarz, H. Hora, M. Labin, and B. Yaakobi (Plenum, New York, 1981), Vol. 5, pp. 253–276.

[21]R. M. More, in Ref. 20, and private communications.

[22]SESAME Library, Los Alamos National Laboratory, Los Alamos, Material No. 3712 (unpublished).

[23]A. Ng, P. Celliers, D. Pasini, J. Kwan, D. Parfeniuk, and L. DaSilva, Phys. Fluids **27**, 2774 (1984).

[24]A. Ng, D. Parfeniuk, and L. DaSilva, Opt. Commun. **53**, 389 (1985).

[25]J. P. Christiansen, D. E. T. F. Ashby, and K. V. Roberts, Comput. Phys. Commun. **7**, 271 (1974).

[26]D. Salzmann, S. Eliezer, A. D. Krumbein, and L. Gitter, Phys. Rev. A **28**, 1738 (1983).

[27]A. Ng, D. Pasini, P. Celliers, D. Parfeniuk, L. DaSilva, and J. Kwan, Appl. Phys. Lett. **45**, 1046 (1984).

[28]A. C. Mitchell and W. J. Nellis, J. Appl. Phys. **52**, 3363 (1981).

[29]B. Ahlborn, L. DaSilva, G. McIntosh, and D. Parfeniuk, to be published.

[30]E. A. McLean, S. H. Gold, J. A. Stamper, R. R. Whitlock, H. R. Griem, S. P. Obenschain, B. H. Ripin, S. E. Bodner, M. J. Herbst, S. J. Gitomer, and M. K. Matzen, Phys. Rev. Lett. **45**, 1246 (1980).

[31]D. L. Book, J. P. Boris, and K. Hain, J. Comput. Phys. **18**, 248 (1975).

[32]Ya. B. Zel'dovich and Yu. P. Raizer, in *Physics of Shock Waves and High Temperature Hydrodynamic Phenomena* (Academic, New York, 1966), Vol. 1, Chap. 7.